ARTICLES

Structure and Stability of Aluminum Hydroxides: A Theoretical Study

Mathieu Digne,[†,‡,§] Philippe Sautet,*[,†,‡] Pascal Raybaud,[§] Hervé Toulhoat,[||] and Emilio Artacho[⊥]

Institut de Recherches sur la Catalyse, Centre National de la Recherche Scientifique, 2 Avenue Albert Einstein, 69626 Villeurbanne Cedex, France, Laboratoire de Chimie Théorique et des Matériaux Hybrides, Ecole Normale Supérieure de Lyon, 46 Allée d'Italie, 69364 Lyon Cedex 07, France, Institut Français du Pétrole, Division Chimie et Physico-chimie appliquées, Département Thermodynamique et Modélisation Moléculaire, 1-4 avenue de Bois-Préau, 92852 Rueil-Malmaison Cedex, France, Institut Français du Pétrole, Direction Scientifique, 1-4 avenue de Bois-Préau, 92852 Rueil-Malmaison Cedex, France, and Department of Earth Sciences, University of Cambridge, Downing Street, Cambridge CB2 3EQ, U.K.

Received: November 14, 2001; In Final Form: March 22, 2002

Aluminum hydroxides are the precursors of metastable aluminas which are used in many applications in industrial catalysis. They constitute a starting point for the understanding of transition processes and structures of metastable transition aluminas. Using first-principle density functional calculations, several polymorphs with different degrees of hydration are simulated: gibbsite, bayerite, diaspore, boehmite, and tohdite. Optimized structures, including cell parameters, atomic positions, and space groups, are calculated and compared with experimental crystallographic data. In some cases, polymorphic structures were found with different orientations for the hydrogen bonds. The study of thermodynamical stability as a function of temperature allows to point out the main tendencies: the higher the temperature, the lower is the degree of hydration of the thermodynamical stable species. Furthermore, calculated limiting temperatures of stability of the various polymorphs are predicted and compared favorably with experimental data available on the transition temperatures.

1. Introduction

Transition aluminas, such as γ-alumina, are widely used in refining industry as catalyst supports.[1] Although many experimental studies have been devoted to these systems, their precise crystal structures remain a matter of investigations. Aluminum hydroxides are the hydrated precursors of transition aluminas. The dehydration process is mainly determined by the structure of the precursor (Figure 1). For instance, starting from the boehmite precursor, the dehydration process leads to the stable α-alumina (corundum) via a great variety of metastable transition aluminas: γ-, δ-, and θ-Al_2O_3. Starting from the bayerite or gibbsite precursor, three other types of transition aluminas, such as η, χ, or κ, are observed on the route toward corundum. However, when diaspore is used as hydroxide precursor, the same process drives directly to the stable corundum phase, avoiding the sequence of metastable transition aluminas. Therefore, the formation of transition aluminas as well as part of their structural properties depend on the type of the starting aluminum hydroxide. This explains why the theoretical study of the structure and energetics of aluminum hydroxides appears to us as a mandatory preliminary step for further investigations the structures of transition aluminas. Aluminum hydroxides exhibit the generic formula (Al_2O_3,xH_2O) where x stands for the degree of hydration. The extreme value, x=0, corresponds to the aluminas' stoichiometry. According to x, different types of hydroxides are distinguished. Experimentally, at least six different aluminum hydroxides are well-identified:

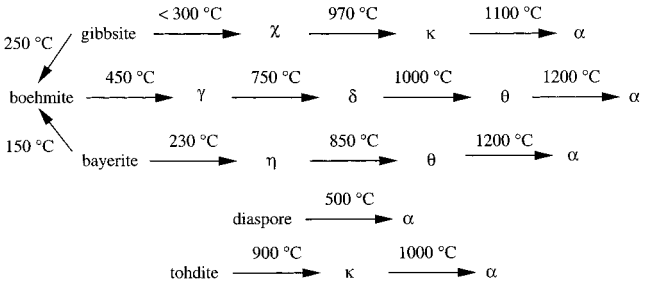

Figure 1. Conversion paths and starting transition temperatures of the different aluminum hydroxides. Aluminas are shown by the associated greek letter. (Adapted from refs 1−4).

- Aluminum trihydroxides $Al(OH)_3$, for which x=3, are gibbsite (γ-$Al(OH)_3$), bayerite (α-$Al(OH)_3$), and nordstrandite.
- Aluminum monohydroxides AlOOH, for which x=1, are boehmite (γ-AlOOH) and diaspore (α-AlOOH).
- A more dehydrated species is tohdite ($5Al_2O_3$,H_2O), corresponding to x=0.2.

Gibbsite, bayerite, diaspore and boehmite are natural solids.[5] For instance, boehmite is the major constituent of many bauxite minerals. All polymorphs can be produced in the laboratory using various methods. Depending on temperature and pH conditions, four of these structures (gibbsite, bayerite, nordstrandite, or boehmite) are obtained by aqueous precipitation

[†] Institut de Recherches sur la Catalyse.
[‡] Laboratoire de Chimie Théorique et des Matériaux Hybrides.
[§] Institut Français du Pétrole, Division Chimie et Physico-chimie appliquée.
[||] Institut Français du Pétrole, Direction Scientifique.
[⊥] Department of Earth Science.

10.1021/jp014182a CCC: $22.00
Published on Web 04/25/2002

of aluminum salts. A mixture of different products is often recovered with more or less amorphous structure.[6] Another route for synthesis is the hydrothermal method. This is the only treatment to obtain tohdite.[7] In this case, water vapor pressure and temperature are the key parameters for controlling the nature of the formed polymorph.

The different polymorphs share several common structural properties: they consist of a well-defined oxygen network, forming interstices. Aluminum atoms are located in these interstices and they are octahedrally coordinated, except in tohdite, where 20% of aluminum atoms are in a tetrahedral environment. The symmetry of the oxygen network governs the type of products formed after dehydration. For instance, the hexagonal ABAB stacking of diaspore leads to the hexagonal α-alumina, whereas the ABC stacking in boehmite layers leads to the faced centered cubic γ-alumina. Finally, the hydrogen bonds present in these compounds play a fundamental role, since they ensure the cohesion of the layered structure of boehmite, gibbsite, or bayerite.

Aluminum hydroxides have been extensively studied by various experimental methods. In particular, X-ray diffraction (XRD) is a well-established method for the determination of the cell shape and of the locations of aluminum and oxygen atoms. However, the positions of the hydrogen atoms, which also determine the space group, remains controversial in many polymorphs. Several not fully conclusive attempts were made by using, on deuterated samples, XRD and neutron diffraction,[8−13] as well as Raman and IR spectroscopies[14,15] or NMR spectroscopy.[16] More recently, theoretical studies have been carried out on diaspore by Winkler et al.,[17,18] on boehmite and gibbsite by Wolverton and Hass,[19] on bayerite and gibbsite by Gale et al.,[20] and on boehmite and diaspore by Rosso and Rustad.[21] The latter study focused on AlOOH stoichiometry and simulated several hypothetical AlOOH polymorphs. Surface and morphology properties of boehmite have been investigated by Raybaud et al.[22] by DFT techniques, whereas the transformation of boehmite into γ-alumina has been also a matter of a theoretical study.[23] The latter two studies put forward the key role of the hydrated precursor for a better description of the final alumina structure.

In the present work, we present the first theoretical study that extends to all hydroxide polymorphs and compares their structural and energetic properties. We describe, in section 2, technical aspects of the ab initio calculations and of the symmetry determination. In section 3, we present the results obtained on the equilibrium geometry of the structures of diaspore, boehmite, bayerite, gibbsite, and tohdite. A particular attention is paid to the influence of hydrogen atoms positions on energetics and geometry. A simple thermodynamical model will bring new insights for explaining the relative stability of the different polymorphs, as a function of the temperature. Either for the structural properties or for the energetics, the results obtained will be compared with data available in the literature.

2. Computational Method

The calculations are based on the density-functional theory, in the standard Kohn−Sham formalism, as implemented in the SIESTA package.[24,25] The exchange-correlation energy is calculated in the framework of the generalized gradient approximation, using the functional proposed by Perdew, Burke, and Ernzernhof.[26] This choice is justified by the fact that the hydrogen bonds are better reproduced by the GGA approach than the LDA approach. Troullier-Martins norm-conserving pseudopotentials,[27] with partial core corrections,[28] are used. The atomic reference configurations are $3s^2 3p^1$ for Al, $2s^2 2p^4$ for O, and $1s^1$ for H. The Kohn−Sham equations are solved by diagonalization of the Hamiltonian matrix and the eigenstates are expanded on a strictly localized basis set.[29] Double-ζ basis functions, plus polarization functions, are used for each atom. The shape of these basis functions are optimized by a simplex method (for more details on this method, see ref 30). The reference structures for this optimization are α-Al_2O_3 in its rhombohedral cell for the Al and O basis sets, and an isolated water molecule for the H basis set. Crystal structures relaxations are performed with periodic boundary conditions. Atomic positions as well as the cell's shape and volume are allowed to be optimized. The structure minimization is carried out by using a conjugate gradient algorithm. According to the convergence criteria, each component of the forces acting on the ions must be lower than 0.04 eV/Å, while the stress tensor acting on the cell must exhibit components lower than 0.2 GPa. The convergence with the size of the **k**-points mesh in reciprocal space was fully tested, and obtained for a **k**-points fineness of 0.1 $Å^{-1}$.

No symmetry conditions were imposed during the relaxation. This means that, during optimization, the space group of the starting configuration is allowed to change within the translational symmetry imposed by the periodic boundary conditions. The space group symmetry of the relaxed structure was determined by using the Symmetry module delivered within the *Cerius*[2] interface.[31] The tolerance was set to 0.01 Å, meaning that each atomic coordinate is allowed to move in an interval of 0.01 Å around the relaxed positions to find the symmetry elements. This precision was determined a posteriori by calculating the maximum displacements of atoms for the five last steps of the geometry relaxation. This maximum length is between 8×10^{-4} Å and 7×10^{-3} Å, depending on the structure studied. Thus, a tolerance of 0.01 Å is reasonable with respect to the numerical determination of equilibrium atomic positions.

The complete relaxed structures, reported in Supporting Information, are given using the Wyckoff notations for the atomic positions: the internal coordinates are written in fractional form for coordinates imposed by the symmetry of the site and in a decimal form including three digits for the calculated ones.

3. Results and Discussion

3.1. Optimized Structures. *Diaspore.* The structure of diaspore is well-known and is not held in any doubt (Figure 2). The simulation of this system is hence an ideal case to test the methodology. The calculated space group is *Pbnm* in agreement with experiments.[11] The atomic positions, reported in Table 1, are close to these determined by DFT-plane wave calculations[18,21] and agree well with experimental values. The simulation of hydrogen bonds is also well rendered by our calculations. Compared with the experimental results (Table 2), the O−H distance and the angle ∠OHO are slightly overestimated (3.6% and 1.3%, respectively), whereas the O···H distance is underestimated of 5.7%. However, this remains within the margin of error of DFT calculations. The good agreement of the structural properties calculated on diaspore (cell volume, shape and parameters) with experimental data can be regarded as a first evidence of the reliability of our methodology (including the choice of the basis functions) for simulating aluminum hydroxides.

Boehmite. Boehmite has the same stoichiometry as diaspore. Its structure has been extensively studied using various methods. XRD or neutron diffraction,[12,13] IR and Raman spectroscopies,[14,15] and NMR spectroscopy[16] determined unambiguously the posi-

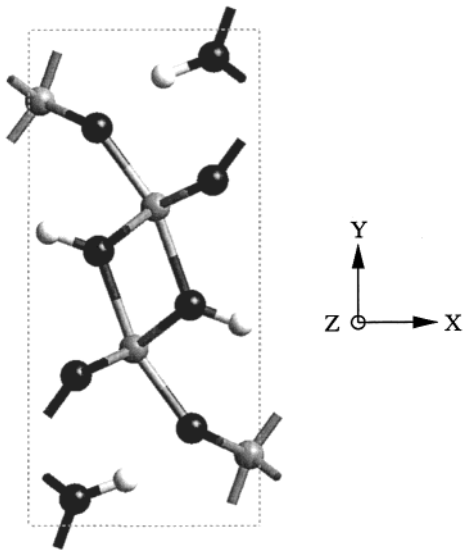

Figure 2. Unit cell of diaspore. Black balls: oxygen atoms. Gray balls: aluminum atoms. White balls: hydrogen atoms.

TABLE 1: Calculated and Experimental Structure of Diaspore

	exptl[a]	calcd
a (Å)	4.401	4.410
b (Å)	9.425	9.527
c (Å)	2.845	2.882
V (Å^3)	118.0	121.6
space group	*Pbnm*	*Pbnm*

[a] Reference 11.

TABLE 2: Structural Parameters for OH Groups Involved in Hydrogen Bonds

	d(O−H) (Å)		*d*(O···H) (Å)		∠OHO (deg)	
compound	exptl	calcd	exptl	calcd	exptl	calcd
diaspore	0.992	1.028	1.705	1.608	160.7	162.8
boehmite	0.928	1.020	1.812	1.611	169.2	178.8
gibbsite	0.838	0.998	1.997	1.763	176.6	167.9
interlayer	0.882	1.001	1.911	1.678	169.7	171.1
	0.861	1.005	2.038	1.790	172.3	166.2
(average)		(1.001)		(1.744)		(168.4)
gibbsite	0.749	0.983	2.472	2.211	149.7	153.2
intralayer	0.773	0.991	2.393	2.155	143.1	140.2
	0.875	0.994	2.207	1.927	148.0	162.5
(average)		(0.989)		(2.098)		(152.0)
bayerite	0.947	0.993	2.024	1.918	169.9	175.8
interlayer	0.963	0.995	1.929	1.917	177.3	175.3
	1.025	0.998	2.007	1.910	162.0	168.3
(average)		(0.978)		(1.915)		(173.1)
bayerite	0.939	0.987	2.276	2.187	138.4	139.4
intralayer	0.966	0.930	2.433	2.360	138.3	146.9
	0.997	0.988	2.106	2.024	152.9	156.8
(average)		(0.987)		(2.190)		(147.7)

tion of aluminum and oxygen atoms. However, incertitudes remain for the precise location of hydrogen atoms. Oxygen and aluminum atoms form a double layer of octahedra, developed in the (*x*Oz) plane and the hydrogen atoms which are between the double layers, generate a zigzag chains of hydrogen bonds along the *Z*-axis. First, we have simulated the simplest model of boehmite, i.e., a unit cell with a four-AlOOH-unit formula in the $Cmc2_1$ symmetry (Figure 3a and Table 3). It enables to show that the lattice parameters and the atomic positions agree reasonably well with experimental data and hydrogen bonds are well-reproduced (Table 2). Experimentally, the periodicity of the chains along the *X*-axis remains unknown. Indeed, each chain presents two possible configurations: O−H···O−H···O and

TABLE 3: Calculated and Experimental Structure of Boehmite

	exptl[a]	calcd
a (Å)	2.876	2.904
b (Å)	12.240	12.069
c (Å)	3.709	3.744
V (Å^3)	130.6	131.2
space group	$Cmc2_1$	$Cmc2_1$

[a] Reference 12.

TABLE 4: Calculated and Experimental Structure of Gibbsite

	exptl[a]	calcd
a (Å)	8.684	8.765
b (Å)	5.078	5.083
c (Å)	9.736	9.594
β	94.54	92.63
V (Å^3)	428.0	427.0
space group	$P2_1/n$	$P2_1/n$

[a] Reference 9.

O···H−O···H−O. If all chains are oriented in the same direction (parallel) along the *X*-axis, the space group should be found equal to $Cmc2_1$ as proposed in ref 12 or in ref 15 (Figure 3b), whereas if their orientation is alternate (antiparallel), the space group should be $P12_1/c1$, as reported in ref 14 (Figure 3c). Finally, if we assume that the two configurations are equivalent and that hydrogen atoms occupy their two possible positions with an equiprobability of 0.5, the centrosymmetric *Cmcm* space group should be found as proposed by refs 13 and 16. Attempting to solve the problem of the hydrogen atoms positions, we have performed the following calculations: we doubled the unit cell size along the *X*-axis and we relaxed the structure with the O−H···O chains parallel ($Cmc2_1$ space group, Figure 3b) and the structure with the O−H···O chains antiparallel ($P12_1/c1$ space group, Figure 3c). The change from one configuration to the other one could occur by hydrogen jumps:

$$\text{O}-\text{H}\cdots\text{O} \rightleftharpoons \text{O}\cdots\text{H}-\text{O} \qquad (1)$$

The antiparallel chains are found to be slightly more stable. However, the energy difference is small (0.2 kJ/(mol AlOOH)), smaller than the intrinsic accuracy of the approximations in the implementation of DFT. This shows that the precise orientation of hydrogen bonds does not modify significantly the total energy of the system. According to ref 23, many hydrogen jumps have been observed during ab initio molecular dynamics simulation at finite temperature. It proves that the barrier energy for hydrogen transfers can be easily overcome by thermal agitations. As a consequence, the space group *Cmcm* in which all the hydrogen sites are equivalent appears as the most probable at ambient temperature.

Gibbsite. The most convincing description of the structure of gibbsite $Al(OH)_3$ was proposed by Saafeld and Wedde[9] using XRD. Gibbsite is a layered compound (Figure 4a): each layer consists of a stacking of AlO_6 octahedra sharing one edge, along the (*x*Oy) plane. Each oxygen atom is linked to one hydrogen atom: half of the hydrogen atoms form intralayer hydrogen bonds in the (*x*Oy) plane and the remainder form interlayer hydrogen bonds along the *Z*-axis, ensuring the cohesion of the gibbsite layers. The parameters given by Saafeld, containing eight $Al(OH)_3$ units per cell and presenting a $P2_1/n$ symmetry, are taken as the starting configuration for the optimization. The relaxed structure presents a nice agreement with the experimental one (Table 4): the symmetry remains unchanged, the cell and the internal positions of aluminum and oxygen atoms

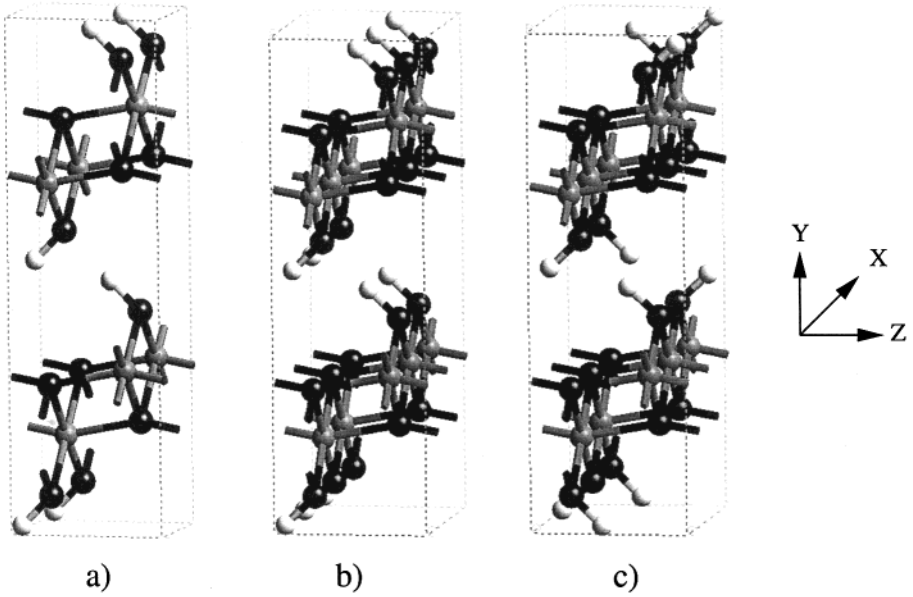

Figure 3. (a) Simplest cell to describe boehmite containing four AlOOH units in the $Cmc2_1$ symmetry. Possible cells of boehmite containing eight AlOOH units: (a) in the $Cmc2_1$ symmetry (the primitive cell is multiplied by two along the *X*-axis), (b) in the $P12_1/c1$ symmetry.

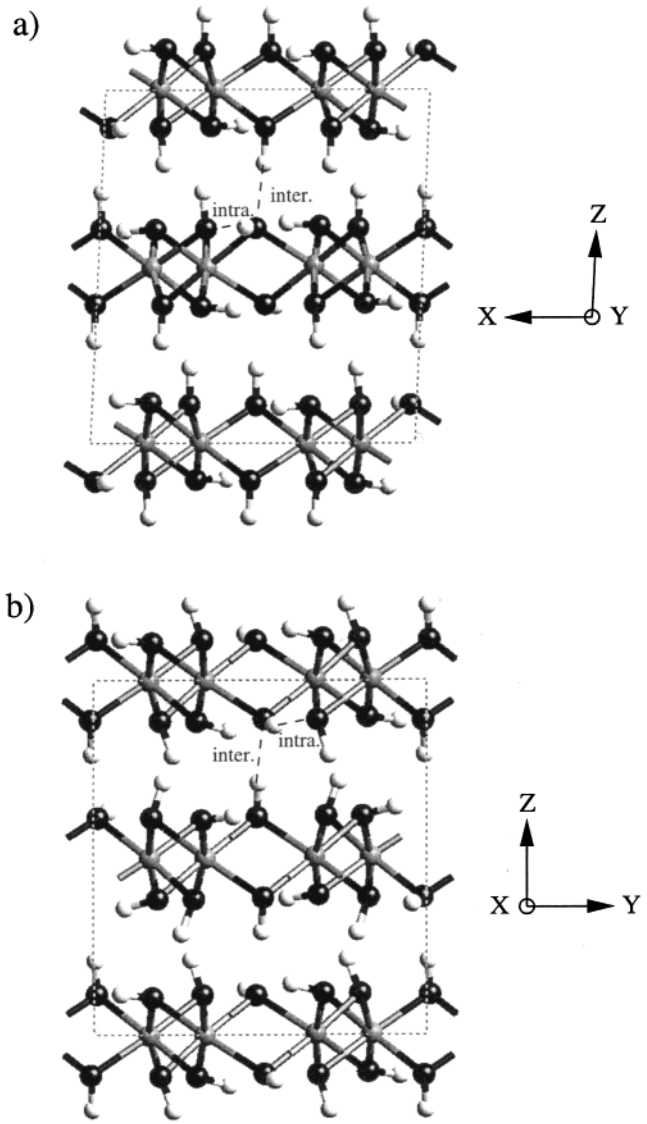

Figure 4. Unit cells of trihydroxides: (a) gibbsite and (b) bayerite. For each structure, one interlayer and one intralayer hydrogen bonds are shown (signified by "inter" and "intra").

are very similar to the experimental data. The important difference for the positions of hydrogen atoms has already been explained by the inaccuracy of XRD to locate these light atoms.[19] Finally, it is noteworthy that hydrogen bonds involved either in the intralayer cohesion or in the interlayer cohesion behave differently (Table 2). The intralayer hydrogen bonds exhibit smaller O−H distances, smaller ∠OHO angles, and larger O···H distances.

Another structural minimum was found very close from the true gibbsite exhibiting the same symmetry and equivalent lattice parameters, but with a smaller β angle (83.33° against 92.63°). It corresponds to a different distribution of intra and interlayer hydrogen bonds. This local minimum is significantly higher in energy of about 15.0 kJ/(mol $Al(OH)_3$), which shows that this structure is metastable and cannot be found at moderate temperature.

At this stage, it is interesting to compare our results with these reported very recently by Gale et al.[20] Using a similar method (SIESTA package), these authors have found for instance a greater cell volume (445.4 Å^3) than ours (427.0 Å^3). Compared to the plane-wave calculation value (434.4 Å^3) or to the experimental value (428.0 Å^3), the agreement is better and we attribute this improvement to the extensive optimization of our basis functions using the corundum structure as reference (see section 2).

Bayerite. Bayerite has the same stoichiometry as gibbsite and exhibits a very similar layered structure (Figure 4b). The main difference consists of the way the interlayer hydrogen bonds are distributed on the two structures. The first precise description of bayerite was obtained by Rothbauer et al.[8] using XRD: a unit cell containing four $Al(OH)_3$ units with a $P2_1/n$ symmetry was found. Later, Zigan et al.,[10] using XRD on deuterated samples, showed that the unit cell is better described if the *c* lattice parameter (direction of the interlayer hydrogens bonds) is doubled, leading to eight $Al(OH)_3$ units per cell. We have tested the two proposed structures which, in fact, do not have the same distribution of intra and interlayer hydrogen bonds. The cell containing four $Al(OH)_3$ units cell relaxed toward a structure with a β angle of 77.72°, which does not match the experimental value of 90.26°. On the contrary, the cell with eight $Al(OH)_3$ units yields a relaxed structure in agreement with

TABLE 5: Calculated and Experimental Structure of Bayerite

	exptl[a]	calcd
a (Å)	5.063	5.091
b (Å)	8.672	8.761
c (Å)	9.425	9.391
β	90.26	90.07
V (Å^3)	413.8	418.8
space group	$P2_1/n$	$P2_1/n$

[a] Reference 10.

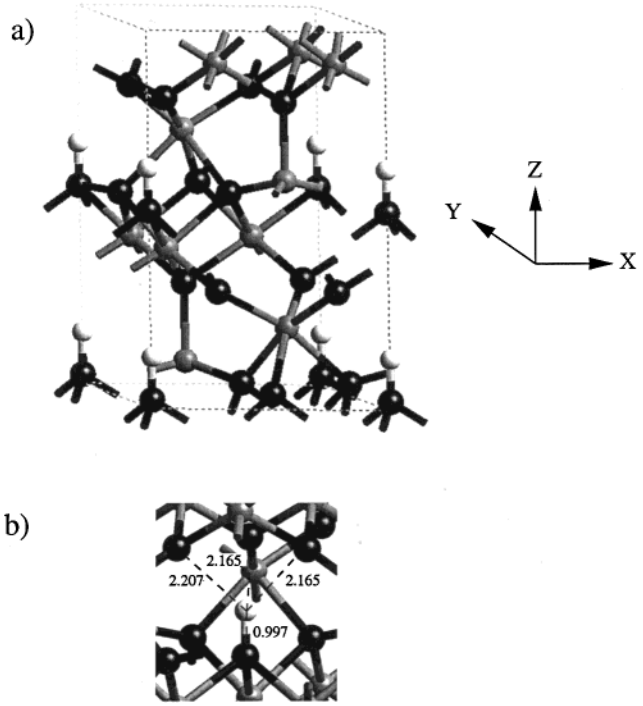

Figure 5. (a) Unit cell of tohdite and (b) tetrahedral site occupied by the hydrogen atom (O−H distances are expressed in angstroms).

experimental values (Table 5). However, the latter structure is stabilized by only 3.8 kJ/(mol $Al(OH)_3$). As they are in gibbsite, the OH distances are slightly different as far as interlayer or intralayer hydrogen bonds are concerned. Furthermore, in the case of bayerite, the calculated O−H distances (Table 2) match the experimental ones, which confirms that the experimental hydrogen positions in gibbsite reported in ref 9 must be rejected. Finally, for the same reasons as in the case of gibbsite, we notice an improvement of the structural properties optimized within our work in comparison with those reported in ref 20.

Tohdite. The structure of tohdite was studied by Yamaguchi et al.[7] They did not succeed in locating hydrogen atoms in the unit cell and they attributed the space group $P6_3mc$ with respect to aluminum and oxygen positions only. Starting from this experimental structure, two hydrogen atoms per cell in the 2*a* or 2*b* Wyckoff positions (Figure 5a) must be added to obtain the correct stoichiometry $[5Al_2O_3,H_2O]$. Furthermore, a careful analysis shows the existence of tetrahedral interstitial sites created by four 3-fold coordinated oxygens along the *Z*-axis of tohdite. One oxygen atom, in C_{3v} symmetry, can easily be linked to an hydrogen atom. In this case, the corresponding hydrogen atoms are in 2*a* positions.

The relevant parameters of the relaxed structure are reported in Table 6. The lattice parameters match well the experimental ones, but the space group differs from experiments: we observe a decrease of the symmetry from $P6_3mc$ to $Cmc2_1$ group. In fact, if we increase the tolerance for the calculation of the space group from 0.010 to 0.055 Å, we recover the initial $P6_3mc$ space group (see Supporting Information). In this case, the internal coordinates for aluminum and oxygen atoms are consistent with the experimental values. Hence, the presence of hydrogen is at the origin of the symmetry lowering. A more precise description of the hydrogen site (Table 7) shows that the surrounding oxygen atoms are not equivalent. The OH distance is 0.997 Å, and for the nonbonded oxygen atoms, two of them are distant of 2.165 Å from the hydrogen, whereas the last one is distant of 2.207 Å (Figure 5b). In a perfect $P6_3mc$ space group, these three oxygen atoms would be equivalent. As a conclusion, the space group $Cmc2_1$ must be attributed to tohdite at 0 K.

TABLE 6: Calculated and Experimental Structure of Tohdite

	exptl[a]	calcd
a (Å)	5.576	5.646
c (Å)	8.768	8.831
V (Å^3)	236.1	244.0
space group	$P6_3mc$	$Cmc2_1$

[a] Reference 7.

TABLE 7: Calculated Structural Parameters for OH Groups in Tohdite and in HAl_5O_8 Spinel

compound	site	*d*(O−H) (Å)	*d*(O···H) (Å)
tohdite	tetra	0.997	2.165
			2.165
			2.207
(average)			(2.179)
HAl_5O_8	tetra	1.002	2.244
			2.301
			2.312
(average)			(2.286)
HAl_5O_8	octa	1.005	2.108
			2.108
			2.426
			2.426
			2.908
(average)			(2.395)

However, we cannot exclude that temperature effects may modify this result. Indeed, the $P6_3mc$ geometry is stabilized by only 1.2 kJ/(mol $[5Al_2O_3,H_2O]$) versus the $Cmc2_1$ geometry. This means that the hydrogen atom can easily move from one configuration to the other, hence leading to an average structure with $P6_3mc$ symmetry. A molecular dynamics simulation, beyond the scope of the present study, should enable to confirm this proposal.

3.2. Phase Stability Diagram. To compare the stability of compounds with different stoichiometries, the following method is adopted: the unit cell of each hydroxide can be written as $[Al_2O_3,xH_2O]$ with *x* varying between 0 and 3. The extreme cases correspond to α-alumina (*x*=0) and to trihydroxides (*x*=3). So, the equilibrium between an hydroxide and α-alumina, which is the high-temperature stable polymorph, can be expressed as

$$\alpha\text{-}Al_2O_3 + xH_2O \rightleftharpoons [Al_2O_3, xH_2O] \qquad (2)$$

and the corresponding variation of the Gibbs free energy is

$$\Delta G(T) = G^{(s)}_{[Al_2O_3,xH_2O]} - G^{(s)}_{\alpha-Al_2O_3} - xG^{(l/g)}_{H_2O} \qquad (3)$$

To estimate eq 3, we use a similar approach as proposed in refs 19 and 23. Assuming that the entropic contributions for the solid phases can be neglected versus the contributions of water, $G^{(s)}_{[Al_2O_3,xH_2O]}$ and $G^{(s)}_{\alpha-Al_2O_3}$ will be approximated by their internal energy calculated at 0 K. The expression of $G^{(l/g)}_{H_2O}$ can be expressed as follows according to *T*. For *T*<373 K,

$$G^{(l/g)}_{H_2O} = E^{(g)}_{H_2O} - \Delta H^{vap}_{H_2O} - TS^{(l)}_{H_2O} \quad (4)$$

$E^{(g)}_{H_2O}$ stands for the internal energy of one isolated water molecule, calculated ab initio, while $\Delta H^{vap}_{H_2O}$ and $S^{(l)}_{H_2O}$ can be found in thermodynamical tables such as those in ref 32. In Table 8, we report the numerical values of ΔG for T=298 K. For T>373 K,

$$G^{(l/g)}_{H_2O} = E^{(g)}_{H_2O} - TS^{(g)}_{H_2O} \quad (5)$$

and the variation of the Gibbs free energy for the reaction 2 is approximated by

$$\Delta G(T) \simeq E^{(s)}_{[Al_2O_3,xH_2O]} - E^{(s)}_{\alpha-Al_2O_3} - xE^{(g)}_{H_2O} + xTS^{(g)}_{H_2O} \quad (6)$$

The diagram drawn in Figure 6 represents the stability domains of each type of polymorph as a function of temperature for T greater than the vaporization temperature of water.

Stability at Ambient Temperature. The values of ΔG(298 K) are reported in Table 8. Several interesting points can be stressed:

•The variations of the Gibbs free energy are negative for all hydroxides, which is consistent with the fact that, at the earth's surface, aluminum is found in the form of hydroxides or oxyhydroxides. The dehydrated species become stable only at high temperature. Furthermore, the higher the degree of hydration, the more stable is the polymorph.

•The Gibbs free energy difference between the two monohydroxides, boehmite and diaspore, is only 3.9 kJ per mole of Al_2O_3. This value is in agreement with the recent calculated value using GGA and Norm conserving pseudopotential of Rosso and Rustad.[21] The experimental values at 298 K are 8.6 kJ/(mol Al_2O_3)[33] and 8.4 kJ/(mol Al_2O_3).[34] Hence, the sign as well as the order of magnitude of this energy difference appear in good agreement with experiments. According to our calculation, gibbsite appears as the most stable phase at ambient T, which is consistent with the fact that gibbsite is the most abundant aluminum hydroxides in Al-rich minerals.[35] The energy difference is larger between the two trihydroxides, gibbsite and bayerite (10.7 kJ/(mol Al_2O_3)). From experimental measurements of Liu et al.,[33] an estimated energy difference of 6.0 kJ/(mol Al_2O_3) (298 K) is found between gibbsite and bayerite, which is again in rather good agreement with our simulation.

• Finally, the O···H distance seems to be an important parameter governing the relative stabilities of the polymorphs for a given degree of hydration. Indeed, the smaller the O···H distances (see average values in Table 2), the more stable is the hydroxide. This rule is true for gibbsite, found more stable than bayerite, as well as for diaspore found more stable than boehmite, although in this second case the difference between the two O···H distances is very small (below accuracy). A possible explanation is that the O···H distances are quantitatively correlated to the strength of the hydrogen bonds and so to the stability.

Stability at High Temperature. The variation of $\Delta G(T)$ is plotted for each polymorph (Figure 6). Each straight line correspond to a given polymorph. For a given T, the lowest value of ΔG gives the stable phase. The inversion temperature, T_{inv}, which stands for the temperature at which the dehydrated form, α-alumina, becomes stable, is reported in Table 8. Except for the diaspore to α-alumina transition which really occurs, these temperatures represent an upper limit for the hydroxide stability. Indeed, the transformation starts at lower temperature

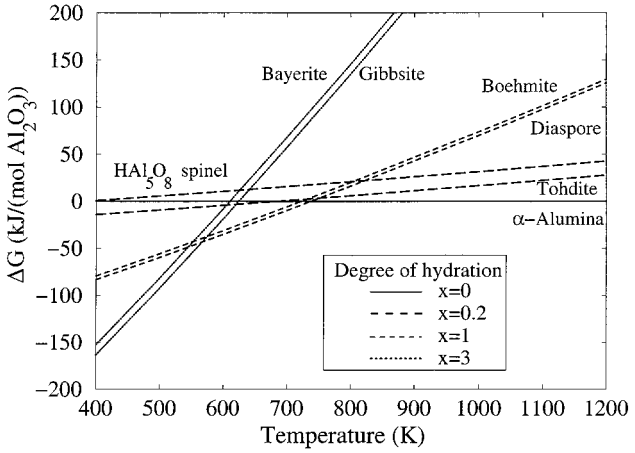

Figure 6. Gibbs free energy of the aluminum hydroxides compared to α-Al_2O_3 (see eq 3), as a function of temperature and for different aluminum hydroxides. The energy is expressed per Al_2O_3 formula unit.

TABLE 8: Thermodynamical Stability of Aluminum Hydroxides (See Text for Definitions)

compound	unit cell $y[Al_2O_3,xH_2O]$	ΔG(298 K) (kJ/(mol Al_2O_3))	T_{inv} (K)	T_{exp}[a] (K)
α-alumina	2[Al_2O_3,0H_2O]	0		
tohdite	5[Al_2O_3,0.2H_2O]	−17.7	698	>900
boehmite	2[Al_2O_3,H_2O]	−97.5	719	>720
diaspore	2[Al_2O_3,H_2O]	−101.4	731	770
bayerite	8[Al_2O_3,3H_2O]	−206.8	609	>500
gibbsite	8[Al_2O_3,3H_2O]	−217.5	624	>570

[a] References 2−4.

(Figure 1) producing metastable transition aluminas, such as η- and γ-alumina. However, the calculated inversion temperature can already bring us new insights on the dehydration process as reported in what follows:

•As expected, when the temperature increases, dehydrated polymorphs become the stable species. An overview of the stability diagram allows to distinguish three main domains. For T below 550 K, the $Al(OH)_3$ polymorphs are stable. For T comprised between 550 and 750 K, AlOOH species become the most stable. Beyond the limit of 750 K, alumina Al_2O_3 is the stable structure.

•Except for tohdite, the calculated inversion temperatures are coherent with the observed transition temperatures. In the case of diaspore for which direct transformation into α-alumina really occurs, the agreement is excellent. The predicted temperature 731 K lies perfectly within the experimental transition interval 680−810 K.[3] The model predicts also that the transition of trihydroxides (bayerite and gibbsite) starts at a lower temperature than for the monohydroxides (boehmite and diaspore) in agreement with experimental values.

•Concerning the stability of tohdite, we do not find any domain of temperature where this compound is stable. This result can be explained by the fact that it is impossible to produce tohdite by simple dehydration at a low water vapor pressure. Only under conditions of hydrothermal synthesis tohdite may be formed:[4] it has been reported that a sample of η-alumina can be inverted into tohdite at T=730 K and P= 300 atm. Furthermore, the upper limit for the existence of tohdite is estimated at about 700 K, which is significantly lower than the transition temperature into κ-alumina (1173 K). A kinetic argument can explain this apparent discrepancy: the structure of tohdite is the only one in which simple hydrogen jumps are not sufficient to generate internal water molecules. Hydrogen atoms have to diffuse into the structure to form H_2O groups,

which will be removed during the calcination. For that reason, an important kinetic barrier has to be overcome to form κ-alumina and could explain why the actual transition temperature is greater than the thermodynamical one estimated by our calculation.

•Lippens and de Boer[36] have already noticed that it is impossible to obtain pure η-alumina from bayerite. Indeed, at the early stage of the calcination, a small amount of bayerite is converted into boehmite. A quantitative experimental study of this phenomena can be found in the work of Zhou and Snyder.[37] Starting from pure bayerite, they follow the calcination process by XRD and DTA. At about 540 K, they observe a mixture of bayerite and boehmite, leading at about 590 K, to a mixture of η-alumina and boehmite. The stability diagram shows that at 552 K, boehmite becomes thermodynamically more stable than bayerite and α-alumina. This explains why there is a competition between a partial dehydration of bayerite into boehmite and a total dehydration into η-alumina which occurs at higher temperature.

•The last relevant question is why bayerite is converted into boehmite and not into diaspore which is energetically more favorable. The presence of a kinetic barrier may explain again that boehmite is formed preferentially to diaspore. Indeed, the oxygen sublattice of diaspore is close to a hexagonal compact lattice, while the one of boehmite and bayerite is close to a face centered cubic one: these compounds lead by dehydration to γ- and η-alumina which are spinel-based structures. Besides, bayerite (as well as gibbsite) is a layered compound, while diaspore (as well as tohdite) is a three-dimensional connected structure. So, from a structural point of view, bayerite is closer to boehmite than to diaspore, which may explain the presence of strong kinetic limitations for the bayerite into diaspore transformation. In the same way, we predict that gibbsite is converted into boehmite at 576 K, i.e., at higher temperature than for bayerite, which is in agreement with experimental observations (Figure 1).

3.3. The HAl_5O_8 Spinel-based Structures. To complete the study of aluminum hydroxides, we have simulated the two HAl_5O_8 spinel-based structures. Indeed, these structures have been recently suggested as a possible candidate for γ- and η-alumina.[38] They can be treated within the same formalism as previously proposed: the stoichiometry $[Al_2O_3,0.2H_2O]$ is the same as tohdite. To form this kind of spinels, in the rhombohedral unit cell of standard spinel $Mg_2Al_4O_8$, we replace the two magnesium atoms by one hydrogen and one aluminum atoms. Two structures can be obtained: the hydrogen atom can be either in a tetrahedral site or in a octahedral site of the original spinel. In the tetrahedral case, we found that the hydrogen atom relaxes in a position different from the ideal tetrahedral position (Table 7): the hydrogen atom forms a covalent bond with one of the oxygen atom and hydrogen bonds with the others. In the octahedral case, the hydrogen atom in the ideal position corresponds to a structural minimum, but we obtain a more stable configuration (Table 7), if a covalent bond is formed with one of the oxygen (energetically, the stabilization is -79.6 kJ/(mol Al_2O_3)). The energy difference between the tetrahedral and octahedral cases is only of 0.7 kJ/(mol Al_2O_3) in favor of the tetrahedral case. This means that, if this kind of compounds exists, they would present hydrogen atoms both in tetrahedral and octahedral sites. However, the comparison of the tetrahedral case with tohdite shows that tohdite is more stable that the hydrogen spinel by -14.9 kJ/(mol Al_2O_3) as reported in Figure 6. The stability of tohdite versus hydrogen spinel can be justified again by analyzing the strength of the hydrogen bonds: the smaller the O···H distance, the more stable the structure. As we explained in the previous section, tohdite does not exhibit a stability domain and hence does not appear during the calcination pathway at reasonable pressure. The situation is even worse for hydrogen spinels which cannot be formed by calcination of boehmite or bayerite. As it was already explained using different arguments,[19] it seems difficult to conceive hydrogen spinel as a good candidates for γ- and η-alumina.

4. Conclusion

This study of various aluminum hydroxides has shown that ab initio approaches are accurate at simulating solids involving hydrogen bonds and to give trends in dehydration processes. The calculated structures are in excellent agreement with experimental ones, even for compounds with low symmetry, which is justified by the quality of the optimized basis functions. These are indeed crucial for obtaining reliable structural and energetic properties of aluminum hydroxides. We have brought new insights concerning the space group symmetry and shown that the total energy of these systems do not depend so much on the precise positions of hydrogen atoms. Energy equivalent structures can be obtained with different orientations of the hydrogen bonds. Calculations of Gibbs enthalpy variations enabled us to explain in a consistent way the thermodynamical stability of hydroxide polymorphs and to predict transition temperatures between $Al(OH)_3$, AlOOH and Al_2O_3. Our approach could be usefully generalized to other families of hydroxides (iron, manganese) naturally abundant and presenting various interests.

Acknowledgment. The authors thank Javier Junquera (Madrid) for his fruitful help and Guillaume Poulet (Lyon) for providing pseudopotentials.

Supporting Information Available: Complete comparisons between experimental and calculated structures. This material is available free of charge via the Internet at http://pubs.acs.org.

References and Notes

(1) Euzen, P.; Raybaud, P.; Krokidis, X.; Toulhoat, H.; Le Loarer, J.-L.; Jolivet, J.-P.; Froidefond, C. Other Oxides and Alumina. In *Handbook of Porous Materials*; Schüth, F., Sing, K., Weitkamp, J., Eds.; Wiley-VCH Verlag GmbH: Weinheim, Germany, 2002; pp 1591−1676.

(2) Cocke, D. L.; Johnson, E. D.; Merrill, R. P. *Catal. Rev.−Sci. Eng.* **1984**, *26*, 163.

(3) Wefers, K.; Misra, C. Alcoa Technical Paper No. 19. Alcoa Laboratories: Pittsburgh, PA, 1987.

(4) Okumiya, M.; Yamaguchi, G.; Yamada, O.; Ono S. *Bull. Chem. Soc. Jpn.* **1971**, *44*, 418.

(5) Levin, I.; Brandon, D. *J. Am. Ceram. Soc.* **1998**, *81*, 1995.

(6) Poisson, R.; Nortier, P.; Brunelle, J. P. In *Catalysts and Supported Catalysts*; Stiles, A. B., Ed.; Butterworths: Boston, 1987; p 11.

(7) Yamaguchi, G.; Yanagida, H. *Bull. Chem. Soc. Jpn.* **1964**, *37*, 1555.

(8) Rothbauer, R.; Zigan, F.; Daniel, H. O. *Z. Kriststallogr.* **1967**, *125*, 317.

(9) Saafeld, H.; Weede, M. *Z. Kristallogr.* **1974**, *139*, 129.

(10) Zigan, F.; Joswig, W.; Burger, N. *Z. Kristallogr.* **1978**, *148*, 255.

(11) Hill, R. J. *Phys. Chem. Miner.* **1979**, *5*, 179.

(12) Christensen, A. N.; Lehmann, M. S.; Convert, P. *Acta Chem. Scand.* **1982**, *36*, 303.

(13) Corbató, C. E.; Tettenhorst, R. T.; Christoph, G. G. *Clays Clay Miner.* **1985**, *33*, 71.

(14) Farmer, V. *Spectrochim. Acta* **1980**, *36A*, 585.

(15) Kiss, A. B.; Keresztury, G.; Farkas, L. *Spectrochim. Acta* **1980**, *36A*, 653.

(16) Slade, R. C. T.; Halstead, T. K. *J. Solid State Chem.***1980**, *32*, 119.

(17) Winkler, B.; Milman, V.; Hennion, B.; Payne, M. C.; Lee, M.-H.; Lin, J. S. *Phys. Chem. Miner.* **1995**, *22*, 461.

(18) Winkler, B.; Hytha, M.; Pickard, C.; Milman, V.; Warren, M.; Segall, M. *Eur. J. Mineral.* **2001**, *13*, 343.

(19) Wolverton, C.; Hass, K. C. *Phys. Rev. B* **2001**, *63*, 24102.
(20) Gale, J. D.; Rohl, A. L.; Milman, V.; Warren, M. C. *J. Phys. Chem. B* **2001**, *105*, 10236.
(21) Rosso, K. M.; Rustad, J. R. *Am. Mineral.* **2001**, *86*, 312.
(22) Raybaud, P.; Digne, M.; Iftimie, R.; Wellens, W.; Toulhoat, H.; Euzen, P. *J. Catal.* **2001**, *201*, 236.
(23) Krokidis, X.; Raybaud, P.; Gobichon, A. E.; Rebours, B.; Euzen, P.; Toulhoat, H. *J. Phys. Chem. B* **2001**, *105*, 5121.
(24) Sánchez-Portal, D.; Ordejón, P.; Artacho, E.; Soler, J. M. *Int. J. Quantum Chem.* **1997**, *65*, 453.
(25) Soler, J. M.; Artacho, E.; Gale, J. D.; García, A.; Junquera, J.; Ordejón, P.; Sánchez-Portal, D. *Condensed Matter* **2001**, paper 0111138.
(26) Perdew, J. P.; Burke, K.; Ernzerhof, M. *Phys. Rev. Lett.* **1996** *77*, 3865.
(27) Troullier, N.; Martins, J. L. *Phys. Rev. B* **1991** *43*, 1993.
(28) Louie, S. G.; Froyen, S.; Cohen, M. L. *Phys. Rev. B* **1982**, *26*, 1738.
(29) Artacho, E.; Sánchez-Portal, D.; Ordejón, P.; García, A.; Soler, J. M. *Phys. Status Solidi b* **1999**, *215*, 809.
(30) Junquera, J.; Paz, O.; Sánchez-Portal, D.; Artacho, E. *Phys. Rev. B* **2001**, *64*, 235111.
(31) *Cerius*^{2} *User Guide;* Molecular Simulations, Inc.: San Diego, 1996.
(32) Lide, D. R., Ed.; *Handbook of Chemistry and Physics*, 76th ed.; CRC Press: New York, 1995−1996.
(33) Liu, P.; Kendelewicz, T.; Brown, G. E., Jr.; Nelson, E. J.; Chambers, S. A. *Surf. Sci.* **1998**, *53*, 417.
(34) Hemingway, B. S.; Sposito, G. In *The Environmental Chemistry of Aluminum*; Sposito, G., Ed.; CRC Press: Boca Raton, 1996; p 81.
(35) Hsu, P. H. In *Minerals in Soil Environnements*; Dixon J. B., Weed, S. B., Eds.; Soil Science Society of America: Madison, WI, 1989; p 331.
(36) Lippens, B. C.; de Boer, J. H. *Acta Crystallogr.* **1964**, *17*, 1312.
(37) Zhou, R. S.; Snyder, R. L. *Acta Crystallogr. B* **1991**, *47*, 617.
(38) Sohlberg, K.; Pennycook, S. J.; Pantelides, S. T. *J. Am. Chem. Soc.* **1999**, *121*, 7493.